TECHNICAL ARTICLE—PEER-REVIEWED

An Experimental Analysis for Damage Monitoring in Glass Fiber/Epoxy Composites During Fatigue Tests by Acoustic Emission

D. Xu · P. F. Liu · Z. P. Chen · S. Q. Zhang

Abstract As a non-destructive technique, Acoustic emission (AE) can be employed to detect the damage inside the material passively and then locate the damage source. However, fatigue loading poses challenges to AE signal acquisition and processing. In this paper, AE monitoring is performed on glass fiber/epoxy composite laminates under fatigue loads. Due to the intrinsic noise, wavelet packet decomposition is used for noise elimination. Results show that the noise components in original AE signals can be effectively eliminated by the wavelet analysis. Based on the difference of the arrival times, the line positioning method is shown to locate AE sources appearing in the laminates successfully. The peak frequency characteristic of each AE signal is utilized for damage mode classification. The fracture of the laminate is governed by delamination and fiber/breakage, followed by fiber/matrix interface debonding.

Keywords Acoustic emission (AE) · Failure analysis · Composite laminates · Fatigue loading

Introduction

As a type of clean and renewable energy, wind energy has shown excellent application prospect under the energy crisis around the world. A high-efficiency system for wind power generation depends largely on the superior performance of wind turbine blades. Now, fiber-reinforced composites achieve successful application in the blade due to its high strength/stiffness and low density. However, severe aerodynamic loads and environments, such as elevated temperature, hygrothermal effects, radiation, lightning, typhoon and storms, can increase the uncertainties of damage initiation, evolution and accumulation in the blade. These conditions subject the blades to a variety of stresses, typically including fatigue, bending, shearing and torsion. Therefore, structural health monitoring (SHM) techniques [1–3] should be used to address damage detection, location and identification so as to avoid the premature failure of the blade.

Due to complex structures of the wind turbine blade, SHM on the blade poses challenges: (1) Conventional testing techniques are time-consuming and labor-intensive because of large sizes of blades, (2) Planar testing methods on surface structures cannot be implemented, (3) Destructive methods undoubtedly affect the remaining lifetime of the blade. By considering the problems above, acoustic emission (AE) is commonly taken as a dynamic non-destructive testing approach and has been widely applied to defect detection of various composite structures [4, 5]. Any subtle damage phenomenon in composite structures can generate an elastic wave, which can be detected by AE sensors and subsequently recorded in the AE apparatus, where such failure modes of fiber failure, matrix cracking, delamination, fiber/matrix interface debonding and shear failure of the adhesive layer are AE sources in composite laminates [6–8] and adhesively-bonded structures [9, 10]. Their characteristics can be identified by AE characteristic features [7, 9, 11, 12], such as the peak amplitude, energy, counts, rise time and time of

D. Xu · Z. P. Chen · S. Q. Zhang
Institute of Chemical Machinery and Process Equipment, School of Energy Engineering, Zhejiang University, Hangzhou 310027, China

P. F. Liu (✉)
Ocean College, Zhejiang University, Zhoushan 316021, China
e-mail: pfliu@zju.edu.cn

duration, or waveform recognition methods [13–15], so as to reflect the damage behaviors of composite structures and to determine weak areas. In this way, damage mode identification can be achieved by leveraging machine learning methods [7, 9, 11, 16, 17] based on some informative AE features. The most used criterion for filtering informative feature is the principal component analysis [7, 9, 11, 16, 17]. Thereafter, the AE characteristics of each damage mode can be derived, dependent on different materials and loads [16–18]. Moreover, the AE technique along with mechanical features allows one to characterize the damage mechanism of composites [19].

Apart from damage mode identification, AE source localization shows significance in AE signal processing, which renders the initial and accumulated damage positions to be determined accurately. Then, detailed damage degree and damage mode in each area can also be determined. However, little research has been performed on the localization of AE sources, compared with damage mode identification. Generally, damage location can be calculated by the difference of arrival time, upon which the same signal reaches different sensors. It is demonstrated that the AE technique can effectively locate the position of AE damage source in the measured composite structure, irrespective of the distance between the source and sensor [20]. For example, fiber breakage in the specimen-scale blade can be detected and located by arranging three AE sensors based on the Time of Arrival (ToA) [21]. Specifically, much attention has been focused on the improvement in positioning accuracy and the corresponding enhancing algorithm in discontinuous structures. It has been shown that the delta-T mapping method [22–24] has superior performance on the source localization in a composite plate with several holes than the ToA method. Combined with the delta-T feature, the least square support vector machine was applicable and accurate in positioning damage in a structure with a lot of inhomogeneities [25]. In addition, the accuracy of damage localization in four-layer composite laminates can be improved after temperature compensation [26]. In summary, these studies above have shed important insight into the source localization and damage mechanisms in small-scale composite structures.

This paper experimentally studies damage source localization and damage mode identification in glass fiber/epoxy composite laminates under fatigue loads by using AE technique. AE monitoring is conducted to collect the AE signals emitted during the whole loading process. After signal acquisition, the wavelet packet decomposition is employed to eliminate the effects of noise in fatigue tests. Comparison between the original signal and the reconstructed signal shows that the noise components in AE signals can be effectively eliminated by the wavelet analysis. The line positioning method is subsequently found to locate AE damage sources in composite laminates successfully. Finally, damage mode identification is achieved by the peak frequency characteristics of AE signals, which is validated by SEM.

Methodology for AE Source Localization

AE source localization cannot be achieved by a single AE sensor. Instead, an array of AE sensors is required such that one AE source can be detected by these sensors. Obviously, ToA for each sensor, i.e., the time it takes for the signal to travel from the source to the sensor, may be different due to different distance between the source and these sensors. In this way, the generated time difference can be utilized to locate the AE source. When it involves complex structures or complicated loads, the accuracy of the ToA method should be tested and validated.

Two commonly used methods, i.e., the line and plane positioning methods, are briefly introduced here. For the former method, at least two AE sensors are required for the source localization. The schematic diagram of the method is shown in Fig. 1a. Given that there is an AE source between Sensors 1 and 2, the location of the source can be determined by different arrival times that it takes for the corresponding elastic wave to spread to different AE sensors, denoted as t_1 and t_2, respectively. The difference between the time intervals can be denoted as $\Delta t = t_1 - t_2$. In this way, the distance from the AE source to Sensor 1 can be calculated as $d = \frac{1}{2}(D - V\Delta t)$, where D and V represent the distance between two sensors and the propagation speed of the AE wave in the detected object, respectively. For the formula above, there are three special locations, i.e., Sensor 1, Sensor 2 and the in-between position, corresponding to time difference of 0, D/V and $- D/V$, respectively. By considering AE sources may be outside the sensor, the time difference is a constant irrespective of the distance between the source and the sensor. Thus, those AE sources will always locate at the position of sensor. It can be concluded that the line positioning method can only be utilized for damage localization in one dimension, i.e., the line between two AE sensors. That is, plane positioning can't be easily achieved by two AE sensors. Indeed, due to the constant value of the distance difference, the potential position of an AE source (X_S, Y_S) can be any point on the hyperbola with its two focuses on the positions of sensors, as shown in Fig. 1b. For a more precise location, it is particularly important to increase the number of AE sensors and to pay attention to sensor arrangement. For example, the plane positioning method by three AE sensors is shown in Fig. 1c. The order of arrival time corresponding to three AE sensors can be

Fig. 1 **a** Line positioning method by two sensors, **b** plane positioning method by two sensors and **c** plane position method by three sensors
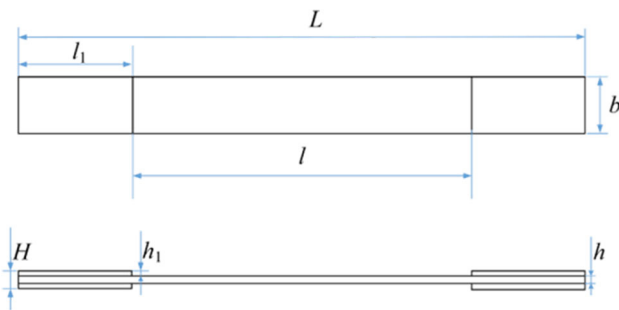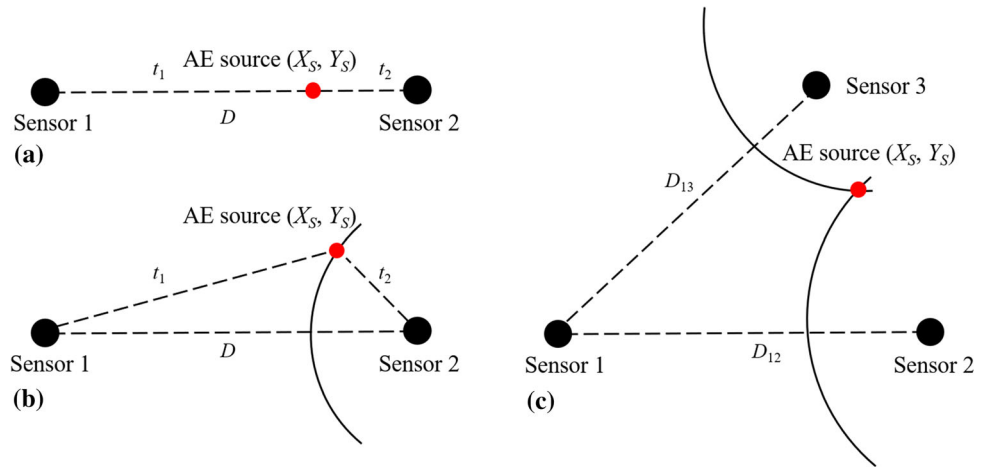

Fig. 2 Geometry of glass fiber/epoxy composite laminates

derived and hence two time-differences can be computed. One hyperbola can be determined by Sensors 1 and 2, and another hyperbola can be determined by Sensors 1 and 3. The intersect of these two curves is the location of the AE source. In this paper, the line positioning method is adopted.

AE Monitoring on Composite Laminates Under Fatigue Loads

The AE monitoring is carried out on two glass fiber/epoxy composite laminates subjected to tension–tension fatigue loads. The fatigue loads vary in a sinusoidal type of waveform with a frequency of about 1 Hz. The maximum load and the minimum load are 63 kN and 6 kN, respectively. The geometry of the specimen with a ply-sequence of $[45°/-45°]_{3s}$ is detailed in Fig. 2, where $L = 200$ mm, $h = 3.3$ mm and $b = 25$ mm represent the effective test length, thickness and width of the specimen, respectively. L_1 and h_1 represent the length and thickness of the stiffener in contact with the fatigue testing machine, respectively. The stiffener is very thin and has almost no effect on the fatigue test. Raw materials of laminates include resin,
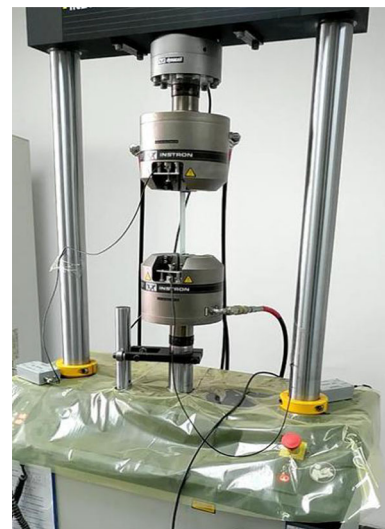

Fig. 3 Fatigue test and AE test on glass fiber/epoxy composite laminates

structural adhesive, glass fiber cloth, core material and polyurethane coating, where resin and structural adhesive are both two-component epoxy resin and the fiber type OCV SE1500 or ECT-468G is employed in main fiber directions of the glass fiber cloth.

By considering the size of the sensor and the geometry of specimen, the effect of AE attenuation in such a small-scale specimen is so weak that it can be neglected. Thus, two piezoelectric AE sensors are selected in this test, with a height of 15 mm and a diameter of 18.8 mm. The diameter of the sensor is close to the width of the specimen. Since the sensor and the signal may be affected by the fractured specimen and the signal attenuation in the metal clamping end is relatively weak, each sensor is fitted with a fixture and then fixed on the machine, as shown in Fig. 3. Due to the effects of vibration from fatigue testing machine on AE signal collection, direct sampling should be performed

2122

J Fail. Anal. and Preven. (2020) 20:2119–2128

Fig. 4 Time (unit: s) versus amplitude (unit: V) for AE waveforms during fatigue tests for **a** specimen-1 and **b** specimen-2
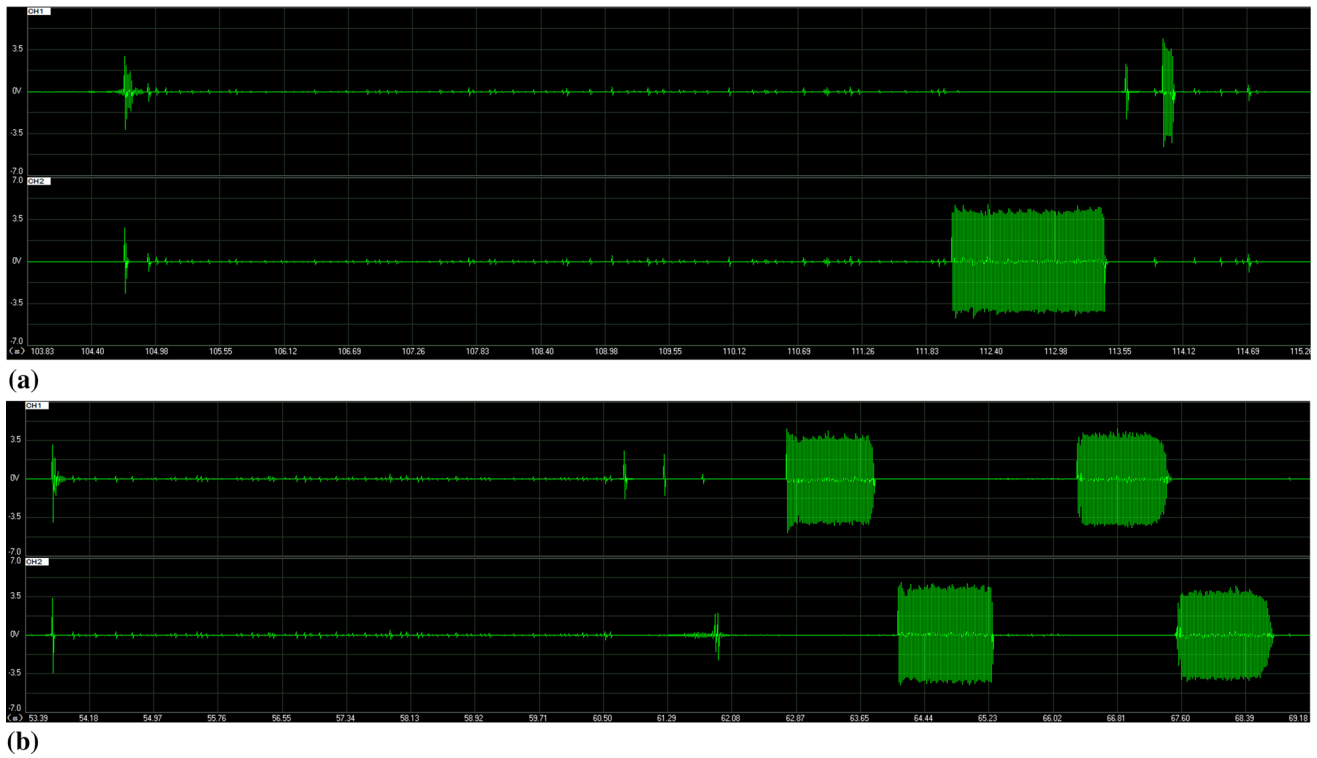

Fig. 5 Time (unit: s) versus amplitude (unit: V) in the time periods for analyzing fracture behaviors of **a** specimen-1 and **b** specimen-2

J Fail. Anal. and Preven. (2020) 20:2119–2128

2123

Fig. 6 **a** The scale function and the wavelet function of the db5 wavelet, **b** the reconstructed signal and the original signal in time domain

Scaling function, N=5

Wavelet, N=5

(a)

Recovered Signal

Noisy Signal

(b)
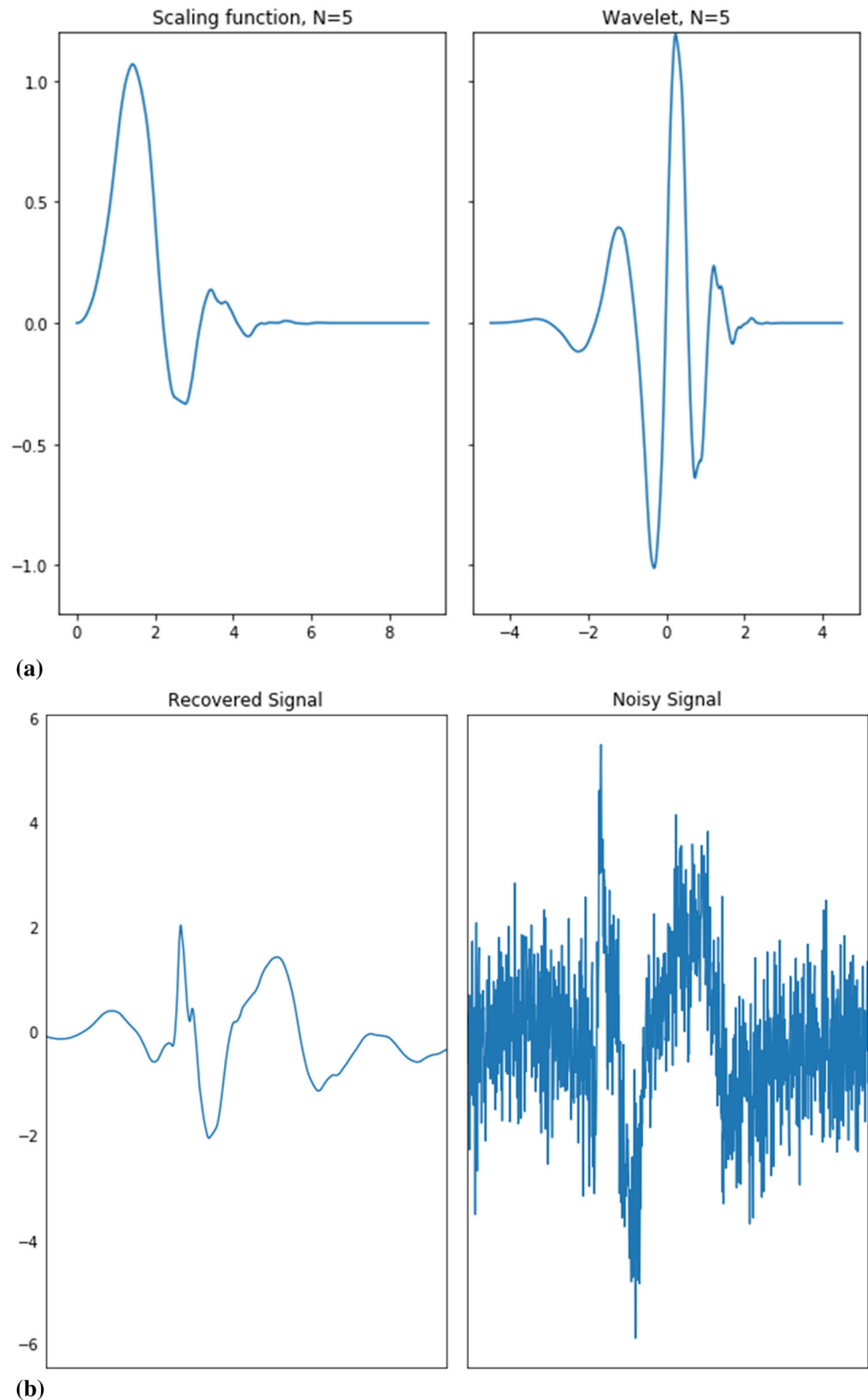
prior to the tension–tension fatigue test such that appropriate threshold value can be set to avoid most of the inherent noise and to guarantee the stability and accuracy of the collected AE signals. In this test, the threshold value is set to 30 mV such that most ambient noise can be eliminated. The preamplifier gain is set to 40 dB. By considering the noise reduction and memory space economization, the intermittent sampling method with the

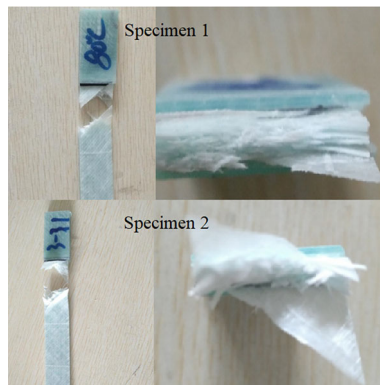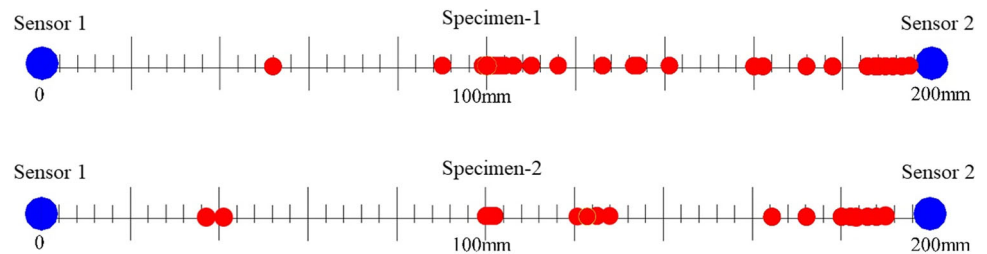Fig. 7 The calculated locations of AE sources in two specimens

Fig. 8 The fracture diagram of each specimen

threshold trigger mode is selected instead of the continuous sampling method. The peak definition time (PDT), the hit definition time (HDT) and the hit lockout time (HLT) are set to 50 μs, 200 μs and 300 μs, respectively.

Before AE signal collection, it is necessary to perform velocity calibration so as to locate AE sources. A type of simulated AE source is required for the generation of stable signals with a wide frequency band. There are many ways to simulate the burst-type AE source, including the laser pulses, the broken glass capillaries and the pencil lead breaks (PLB). In this work, PLB test is adopted and repeated for three times. Specifically, the simulated AE source signal is emitted by the 0.5 HB pencil with a lead length of 2.5 mm and the lead is broken at the angle of 30° with the measured blade surface. The peak amplitude in each PLB test exceeds 95 dB, indicating well-defined AE signals. And the location where the pencil lead breaks is well-located.

Results

The numbers of cycles for specimen-1 and specimen-2 are 61364 and 62245, respectively. Since the sampling mode is intermittent sampling, the total sampling times for these two specimens are 115.34 s and 69.47 s, respectively. As shown in Fig. 4, the AE waveforms in the early and middle stages are dynamically stable, whose amplitudes does not appear to increase explosively. Despite the existence of

transient signals in the early stage, their amplitudes are relatively low. However, a great number of damage signals burst out prior to the ultimate failure of the specimens, with their amplitudes exceeding 3500 mV, as shown in Fig. 4. Therefore, only the later signal segments are taken into consideration for further damage analysis. As shown in Fig. 5, the time periods for analyzing fracture behaviors of specimen-1 and specimen-2 are 11.45 s and 15.79 s, respectively.

In AE tests, the signal strength of AE source originated from the specimen is generally weak and there exist the ambient noise and the noise of acquisition system. Although the ambient noise has been greatly eliminated by setting an appropriate threshold value, the noise of acquisition system cannot be neglected, especially for fatigue tests [27, 28]. Therefore, useful AE signals need to be extracted from the original signals to eliminate noise signals such that damage mode identification and damage source localization can be achieved effectively and reliably. Noise reduction is an essential step in the process of acoustic emission signal processing so as to improve the signal-to-noise ratio.

Signal denoising methods typically include the time domain analysis methods, the frequency domain analysis methods and the time–frequency analysis methods [29]. The time–frequency analysis methods mainly reduce noise through wavelet analysis. Simple denoising methods, such as the median filtering, the mean filtering and the amplitude-limiting filtering, can only eliminate impulse interference caused by accidental factors while fail to cope with complex noise. At present, the wavelet analysis and independent component analysis are two commonly used effective noise reduction methods, where the wavelet analysis has been widely used by many scholars [28, 30, 31]. The process is generally divided into three steps: (1) the appropriate wavelet basis function and the number of the decomposition layer are selected, (2) the wavelet coefficients of each layer are processed and (3) the denoised signal by inverse wavelet transform is reconstructed.

In this work, the wavelet threshold denoising method is used to reduce the noise components in the acquired AE signals. Since results are expectable to differ in the wavelet

packet functions for analyzing the same signal, the choice of the appropriate wavelet packet function is the prerequisite for subsequent signal processing. Among multiple types of wavelet packet functions. The Daubechies series wavelets, the Coif series wavelets and the Symlet series wavelets are more in line with the characteristics of AE signals, which are widely used in AE signal processing. The most commonly used Daubechies series wavelets are selected for noise reduction, specifically the db5 wavelet.

Table 1 The numbers of the burst AE signals in each frequency range for specimen-1

Channels	30–190 (kHz)	200–320 (kHz)	350–500 (kHz)	> 500 (kHz)	Total
1	0	60	231	11	302
2	1	12	126	15	154

Table 2 The numbers of the burst AE signals in each frequency range for specimen-2

Channels	30–190 (kHz)	200–320 (kHz)	350–500 (kHz)	> 500 (kHz)	Total
1	0	29	166	16	211
2	0	38	374	20	432

The scale function and wavelet function are shown in Fig. 6a. By comparing the reconstructed signal with the primary noise-contained signal, the noise components in the original AE signal can be effectively eliminated by employing the wavelet analysis, as shown in Fig. 6b.

The positions of the AE sources acquired from two specimens are calculated by using the line positioning method, as shown in Fig. 7. In comparison with the fracture position of each specimen in Fig. 8, it is found that a great number of positioning events gather at the fracture position of the specimen, where the number of events exceeds half of the total number. Other positioning events are distributed in the remaining part of the specimen. That is, the damage source location evaluated by the AE technique is consistent with the actual fracture position of the specimen. Therefore, it is deduced that the line positioning method based on the ToA method can be used to determine the location of an AE source effectively, corresponding to the initial damage or the evolutionary damage in the specimen.

After damage source localization, the fast Fourier transform is applied to both the burst signal and the continuous signal during the later stage so as to further explore the damage mechanisms which are responsible for the specimen failure. Taking specimen-1 for example, the dominant frequency of the burst signal is within a range of 300–400 kHz, as shown in Fig. 9a. It can be seen from

Fig. 9 The frequency spectrum of damage source for specimen-1 in the later stage: **a** the burst signal, **b** the continuous signal
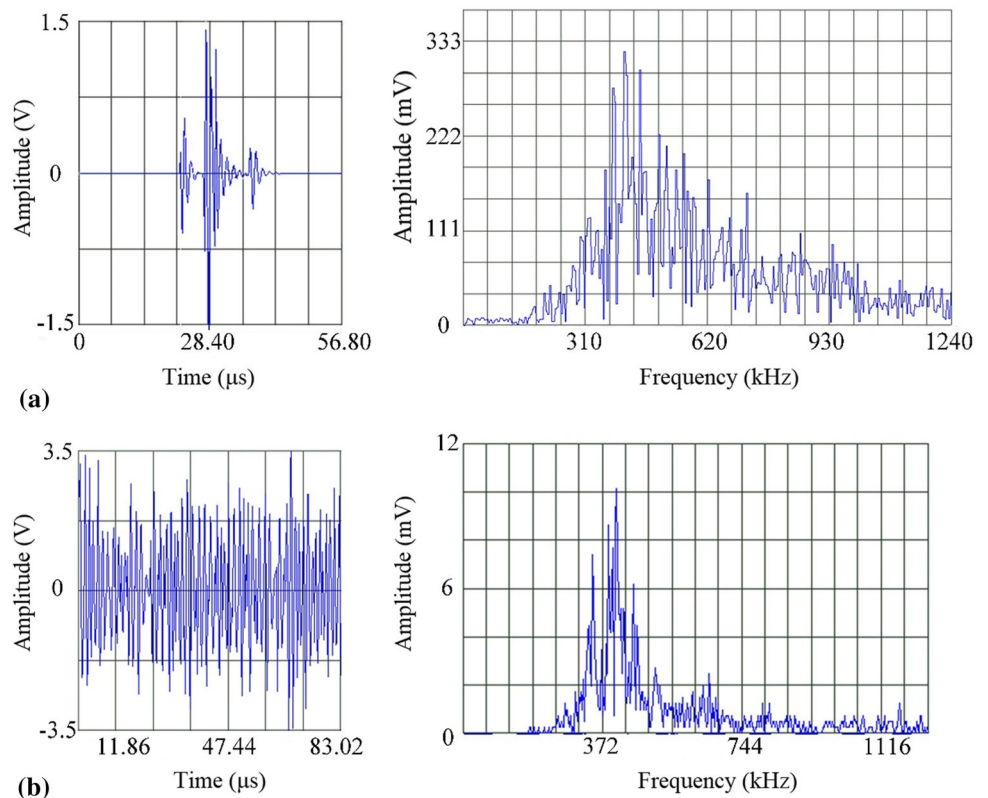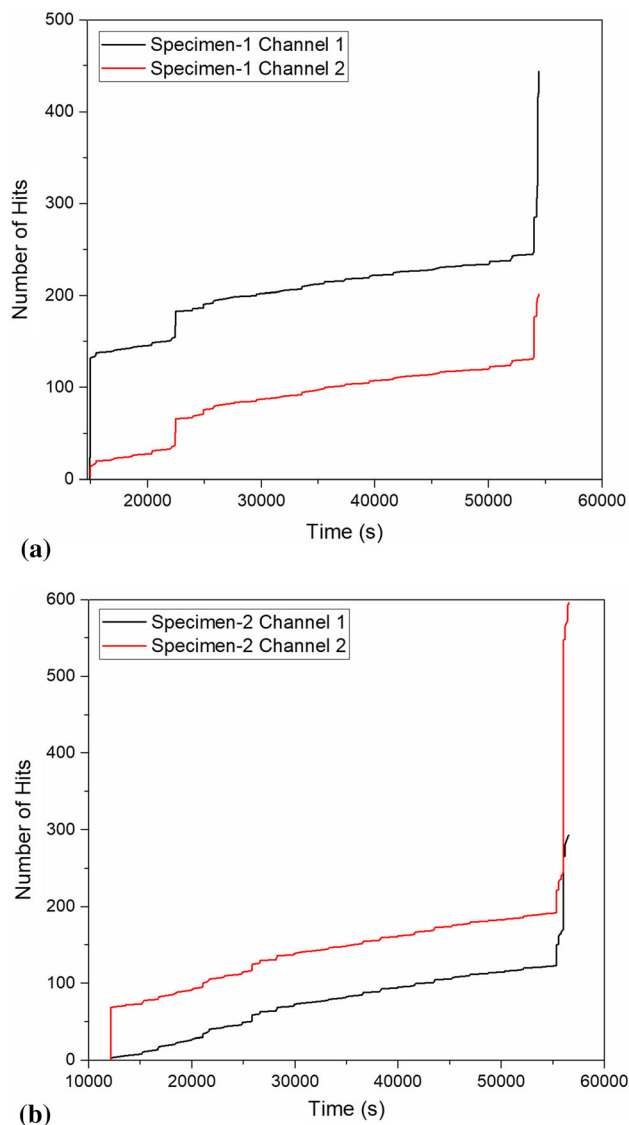
Fig. 10 The increasing number of hits for **a** specimen-1 and **b** specimen-2

Fig. 9b that the frequency features of damage sources corresponding to the later continuous signals are more concentrated in the range of 300–500 kHz. According to a great deal of previous work in glass fiber/epoxy composites [32–36], the ranges of the peak frequency for common damage modes (matrix cracking, matrix/fiber interface debonding, fiber breakage and delamination) are 30–190 kHz, 200–320 kHz and 350–500 kHz, respectively. Thus, in the later stage, it can be deduced that the failure mechanism is mainly manifested as delamination and fiber breakage. Furthermore, the peak frequencies of all burst signals in the later stages for specimen-1 and specimen-2 are grouped into different ranges, with the results listed in

Tables 1 and 2, respectively. The number of AE signals corresponding to delamination and fiber breakage is much more than that of other damage modes. Delamination and fiber breakage are two dominant damage modes during the final fracture process, which can also be visually observed through the fracture appearance of specimen-1 and specimen-2, as shown in Fig. 8. Such a phenomenon is consistent with the frequency concentration in Fig. 9. Thus, it can be deduced that the failure of specimens under fatigue loads is governed by delamination and fiber breakage. The numbers of signals recorded by sensor 1 and sensor 2 are quite different. Specifically, the larger one is about twice as large as the other one. Thus, it is implied that the fracture position is deviated from the center line of the specimen, as exemplified in Fig. 8. The increasing number of hits for each specimen is further shown in Fig. 10. It can be seen the increase in the number of hits is almost a linear function of the fatigue time, except for a few moments of sudden increase. These moments indicate the damage accumulation has reached a new stage, leading to the signal explosion. As can be seen in Fig. 10, prior to the fracture of the specimen, the number of burst signals presents a sharp increase for each channel, which implies the failure of the specimen.

By performing scanning electron microscopy (SEM) on the fracture surface of specimen-1, matrix cracking and fiber/matrix interface debonding can also be clearly seen, as shown in Fig. 11. Matrix cracking and fiber/matrix interface debonding are likely active in the initial stage as shown in Fig. 4 while AE activity are slightly weaker than delamination and fiber breakage during the later stage. Thus, matrix cracking and fiber/matrix interface debonding can be identified as two fundamental damage modes for composites, in agreement with previous research [37, 38].

Concluding Remarks

This paper experimentally monitors the fracture process of glass fiber/epoxy laminates under fatigue loads by using the AE technique. AE signal processing is conducted after initial noise reduction, which is accomplished by the wavelet packet decomposition. Many AE signals are calculated to be clustered at the actual fracture position of the specimen. The peak frequency characteristics of various damage modes are determined. The intensity of AE activity for each damage mode is further investigated. The failure process of specimens is governed by delamination and fiber breakage, followed by less-active fiber/matrix interface debonding. Matrix cracking and fiber/matrix interface debonding are shown to be two basic damage modes that can be easily activated by lower loads.

Fig. 11 Damage modes in the fracture position of specimen-1 by SEM
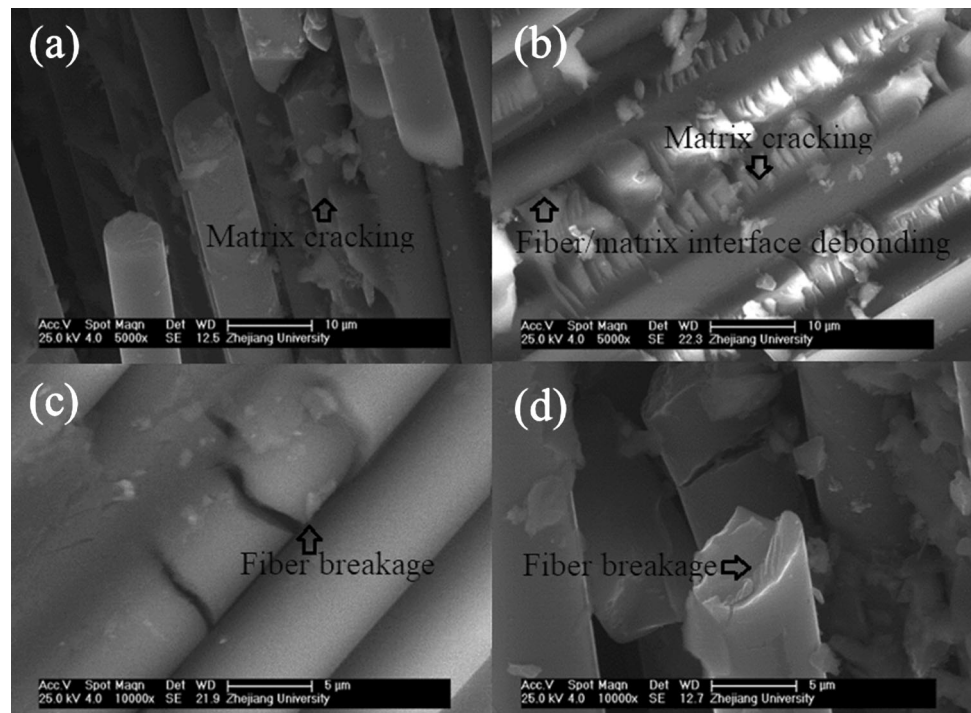
References

1. N. Beganovic, D. Söffker, Structural health management utilization for lifetime prognosis and advanced control strategy deployment of wind turbines: an overview and outlook concerning actual methods, tools, and obtained results. Renew. Sustain. Energy Rev. **64**, 68–83 (2016)
2. R. Yang, Y. He, H. Zhang, Progress and trends in nondestructive testing and evaluation for wind turbine composite blade. Renew. Sustain. Energy Rev. **60**, 1225–1250 (2016)
3. D. Li, S.C.M. Ho, G. Song, L. Ren, H. Li, A review of damage detection methods for wind turbine blades. Smart Mater. Struct. **24**(3), 033001 (2015)
4. H.F. Zhou, H.Y. Dou, L.Z. Qin, Y. Chen, Y.Q. Ni, J.M. Ko, A review of full-scale structural testing of wind turbine blades. Renew. Sustain. Energy Rev. **33**, 177–187 (2014)
5. G. Romhány, T. Czigány, J. Karger-Kocsis, Failure assessment and evaluation of damage development and crack growth in polymer composites via localization of acoustic emission events: a review. Polym. Rev. **57**(3), 397–439 (2017)
6. M. Haggui, A. El Mahi, Z. Jendli, A. Akrout, M. Haddar, Static and fatigue characterization of flax fiber reinforced thermoplastic composites by acoustic emission. Appl. Acoust. **147**, 100–110 (2019)
7. H. Sayar, M. Azadi, A. Ghasemi-Ghalebahman, S.M. Jafari, Clustering effect on damage mechanisms in open-hole laminated carbon/epoxy composite under constant tensile loading rate, using acoustic emission. Compos. Struct. **204**, 1–11 (2018)

8. P.F. Liu, J.K. Chu, Y.L. Liu, J.Y. Zheng, A study on the failure mechanisms of carbon fiber/epoxy composite laminates using acoustic emission. Mater. Des. **37**, 228–235 (2012)
9. D. Xu, P.F. Liu, J.G. Li, Z.P. Chen, Damage mode identification of adhesive composite joints under hygrothermal environment using acoustic emission and machine learning. Compos. Struct. **211**, 351–363 (2019)
10. M. Assarar, M. Bentahar, A. El Mahi, R. El Guerjouma, Monitoring of damage mechanisms in sandwich composite materials using acoustic emission. Int. J. Damage Mech **24**(6), 787–804 (2014)
11. A.R. Oskouei, H. Heidary, M. Ahmadi, M. Farajpur, Unsupervised acoustic emission data clustering for the analysis of damage mechanisms in glass/polyester composites. Mater. Des. **37**, 416–422 (2012)
12. P.F. Liu, J. Yang, X.Q. Peng, Delamination analysis of carbon fiber composites under hygrothermal environment using acoustic emission. J. Compos. Mater. **51**(11), 1557–1571 (2017)
13. M. Chai, Z. Zhang, Q. Duan, A new qualitative acoustic emission parameter based on Shannon's entropy for damage monitoring. Mech. Syst. Signal Proc. **100**, 617–629 (2018)
14. Z. Yang, W. Yan, L. Jin, F. Li, Z. Hou, A novel feature representation method based on original waveforms for acoustic emission signals. Mech. Syst. Signal Proc. **135**, 106365 (2020)
15. W. Guo, B. Li, S. Shen, Q. Zhou, An intelligent grinding burn detection system based on two-stage feature selection and stacked sparse autoencoder. Int. J. Adv. Manuf. Technol. **103**(5–8), 2837–2847 (2019)
16. L. Li, Y. Swolfs, I. Straumit, X. Yan, S.V. Lomov, Cluster analysis of acoustic emission signals for 2D and 3D woven carbon fiber/epoxy composites. J. Compos. Mater. **50**(14), 1921–1935 (2015)
17. H. Heidary, N.Z. Karimi, M. Ahmadi, A. Rahimi, A. Zucchelli, Clustering of acoustic emission signals collected during drilling process of composite materials using unsupervised classifiers. J. Compos. Mater. **49**(5), 559–571 (2014)

2128

J Fail. Anal. and Preven. (2020) 20:2119–2128

18. L. Li, X. Yan, Progressive damage analysis for cross-ply graded PE/PE composites based on cluster analysis of acoustic emission signals. J. Thermoplast. Compos. Mater. **31**(5), 634–656 (2017)

19. A.A.B. Davijani, M. Hajikhani, M. Ahmadi, Acoustic emission based on sentry function to monitor the initiation of delamination in composite materials. Mater. Des. **32**(5), 3059–3065 (2011)

20. X. Lin, G. Chen, J. Li, F. Lu, S. Huang, X. Cheng, Investigation of acoustic emission source localization performance on the plate structure using piezoelectric fiber composites. Sens. Actuator A Phys. **282**, 9–16 (2018)

21. C. Gómez Muñoz, M.F. García, A new fault location approach for acoustic emission techniques in wind turbines. Energies **9**(1), 40 (2016)

22. S.K. Al-Jumaili, M.R. Pearson, K.M. Holford, M.J. Eaton, R. Pullin, Acoustic emission source location in complex structures using full automatic delta T mapping technique. Mech. Syst. Signal Proc. **72–73**, 513–524 (2016)

23. M.J. Eaton, R. Pullin, K.M. Holford, Acoustic emission source location in composite materials using Delta T Mapping. Compos. Part A Appl. Sci. Manuf. **43**(6), 856–863 (2012)

24. J.P. McCrory, S.K. Al-Jumaili, D. Crivelli, M.R. Pearson, M.J. Eaton, C.A. Featherston et al., Damage classification in carbon fibre composites using acoustic emission: a comparison of three techniques. Compos. Part B Eng. **68**, 424–430 (2015)

25. K.R. Kim, Y.S. Lee, Acoustic emission source localization in plate-like structures using least-squares support vector machines with delta t feature. J. Mech. Sci. Technol. **28**(8), 3013–3020 (2014)

26. C. Fendzi, M. Rébillat, N. Mechbal, M. Guskov, G. Coffignal, A data-driven temperature compensation approach for Structural Health Monitoring using Lamb waves. Struct. Health Monit. **15**(5), 525–540 (2016)

27. D.D. Doan, E. Ramasso, V. Placet, S. Zhang, L. Boubakar, N. Zerhouni, An unsupervised pattern recognition approach for AE data originating from fatigue tests on polymer-composite materials. Mech. Syst. Signal Proc. **64–65**, 465–478 (2015)

28. M. Kharrat, E. Ramasso, V. Placet, M.L. Boubakar, A signal processing approach for enhanced acoustic emission data analysis in high activity systems: application to organic matrix composites. Mech. Syst. Signal Proc. **70–71**, 1038–1055 (2016)

29. L. Zhen, H. Zhengjia, Z. Yanyang, W. Yanxue, Customized wavelet denoising using intra- and inter-scale dependency for bearing fault detection. J. Sound Vib. **313**(1–2), 342–359 (2008)

30. E. Douka, S. Loutridis, A. Trochidis, Crack identification in plates using wavelet analysis. J. Sound Vib. **270**(1–2), 279–295 (2004)

31. S. Loutridis, E. Douka, L.J. Hadjileontiadis, A. Trochidis, A two-dimensional wavelet transform for detection of cracks in plates. Eng. Struct. **27**(9), 1327–1338 (2005)

32. R. Mohammadi, M.A. Najafabadi, M. Saeedifar, J. Yousefi, G. Minak, Correlation of acoustic emission with finite element predicted damages in open-hole tensile laminated composites. Compos. Part B Eng. **108**, 427–435 (2017)

33. W. Zhou, W.-Z. Zhao, Y.-N. Zhang, Z.-J. Ding, Cluster analysis of acoustic emission signals and deformation measurement for delaminated glass fiber epoxy composites. Compos. Struct. **195**, 349–358 (2018)

34. C. Yilmaz, C. Akalin, I. Gunal, H. Celik, M. Buyuk, A. Suleman et al., A hybrid damage assessment for E-and S-glass reinforced laminated composite structures under in-plane shear loading. Compos. Struct. **186**, 347–354 (2018)

35. J.L. Tang, S. Soua, C. Mares, T.H. Gan, A pattern recognition approach to acoustic emission Data originating from fatigue of wind turbine blades. Sensors **17**(11), 2507 (2017)

36. M. Fotouhi, H. Heidary, M. Ahmadi, F. Pashmforoush, Characterization of composite materials damage under quasi-static three-point bending test using wavelet and fuzzy C-means clustering. J. Compos. Mater. **46**(15), 1795–1808 (2012)

37. W. Roundi, A. El Mahi, A. El Gharad, J.L. Rebiere, Acoustic emission monitoring of damage progression in glass/epoxy composites during static and fatigue tensile tests. Appl. Acoust. **132**, 124–134 (2018)

38. D.S. de Vasconcellos, F. Touchard, L. Chocinski-Arnault, Tension–tension fatigue behaviour of woven hemp fibre reinforced epoxy composite: a multi-instrumented damage analysis. Int. J. Fatigue **59**, 159–169 (2014)